Global Change Biology
celebrating 20 years

Global Change Biology (2014), doi: 10.1111/gcb.12671

Influence of physiological phenology on the seasonal pattern of ecosystem respiration in deciduous forests

MIRCO MIGLIAVACCA[1,2], MARKUS REICHSTEIN[1], ANDREW D. RICHARDSON[3], MIGUEL D. MAHECHA[1], EDOARDO CREMONESE[4], NICOLAS DELPIERRE[5], MARTA GALVAGNO[4], BEVERLY E. LAW[6], GEORG WOHLFAHRT[7], T. ANDREW BLACK[8], NUNO CARVALHAIS[1,9], GUIDO CECCHERINI[10], JIQUAN CHEN[11,12], NADINE GOBRON[10], ERNEST KOFFI[10], J. WILLIAM MUNGER[13], OSCAR PEREZ-PRIEGO[1], MONICA ROBUSTELLI[10], ENRICO TOMELLERI[14] and ALESSANDRO CESCATTI[10]

[1]*Max Planck Institute for Biogeochemistry, PO Box 100164, Jena 07701, Germany,* [2]*Remote Sensing of Environmental Dynamics Lab, DISAT, University of Milano-Bicocca, P.zza della Scienza 1, Milan, Italy,* [3]*Department of Organismic and Evolutionary Biology, Harvard University, Cambridge, MA 02138, USA,* [4]*Regional Agency for Environmental Protection Valle d'Aosta (ARPA), Aosta, Italy,* [5] *UMR 8079 Ecologie Systematique et Evolution, Universite Paris-Sud, Orsay F-91405, France,* [6]*Department of Forest Ecosystems and Society, Oregon State University, 321 Richardson Hall, Corvallis, OR 97331, USA,* [7]*Institute for Ecology, University of Innsbruck, Sternwartestr. 15, Innsbruck 6020, Austria,* [8]*Biometeorology and Soil Physics Group, Faculty of Land and Food Systems, University of British Columbia, Vancouver, BC V6T 1Z4, Canada,* [9]*Departamento de Ciencias e Engenharia do Ambiente, DCEA, Faculdade de Ciências e Tecnologia, FCT, Universidade Nova de Lisboa, Monte da Caparica, Portugal,* [10]*Institute for Environment and Sustainability, Climate Risk Management Unit, European Commission, Joint Research Centre, Ispra, VA, Italy,* [11]*International Center for Ecology, Meteorology and Environment (IceMe), Nanjing University of Information Science and Technology, Nanjing 210044, China,* [12]*CGCEO/Geography, Michigan State University, East Lansing, MI 48823, USA,* [13]*Division of Engineering and Applied Science/Department of Earth and Planetary Science, Harvard University, Cambridge, MA 02138, USA,* [14]*Institute for Applied Remote Sensing, EURAC, Bolzano, Italy*

Abstract

Understanding the environmental and biotic drivers of respiration at the ecosystem level is a prerequisite to further improve scenarios of the global carbon cycle. In this study we investigated the relevance of physiological phenology, defined as seasonal changes in plant physiological properties, for explaining the temporal dynamics of ecosystem respiration (R_{ECO}) in deciduous forests. Previous studies showed that empirical R_{ECO} models can be substantially improved by considering the biotic dependency of R_{ECO} on the short-term productivity (e.g., daily gross primary production, GPP) in addition to the well-known environmental controls of temperature and water availability. Here, we use a model-data integration approach to investigate the added value of physiological phenology, represented by the first temporal derivative of GPP, or alternatively of the fraction of absorbed photosynthetically active radiation, for modeling R_{ECO} at 19 deciduous broadleaved forests in the FLUXNET La Thuile database. The new data-oriented semiempirical model leads to an 8% decrease in root mean square error (RMSE) and a 6% increase in the modeling efficiency (EF) of modeled R_{ECO} when compared to a version of the model that does not consider the physiological phenology. The reduction of the model-observation bias occurred mainly at the monthly time scale, and in spring and summer, while a smaller reduction was observed at the annual time scale. The proposed approach did not improve the model performance at several sites, and we identified as potential causes the plant canopy heterogeneity and the use of air temperature as a driver of ecosystem respiration instead of soil temperature. However, in the majority of sites the model-error remained unchanged regardless of the driving temperature. Overall, our results point toward the potential for improving current approaches for modeling R_{ECO} in deciduous forests by including the phenological cycle of the canopy.

Keywords: deciduous forests, ecosystem respiration, eddy covariance, FLUXNET La Thuile database, land–atmosphere fluxes, phenology

Received 22 October 2013; revised version received 12 June 2014 and accepted 18 June 2014

Correspondence: Mirco Migliavacca, tel. +49 3641 576281, fax +49 3641 577200, e-mail: mmiglia@bgc-jena.mpg.de

Introduction

The integrated respiration fluxes of terrestrial ecosystems (i.e., 'ecosystem respiration' R_{ECO}) represent a large flux in the global carbon cycle. Hence, to model

climate–carbon cycle interactions, it is important to understand the responses of R_{ECO} to environmental conditions and biotic controls (Davidson & Janssens, 2006; Trumbore, 2006; Mahecha *et al.*, 2010a). However, the processes and complex interactions between the different drivers controlling R_{ECO} are still not fully understood and the associated uncertainty continues to hamper bottom upscaling to regional and continental scales.

Temporal changes of R_{ECO} are partly controlled by the seasonal variability of environmental factors, in particular temperature, soil moisture or precipitation. In addition, empirical studies have demonstrated a tight link between gross primary production (GPP) and R_{ECO} for most ecosystems (e.g., Mahecha *et al.*, 2010a; Peichl *et al.*, 2013). These findings indicate that the seasonal variability of R_{ECO} is partially dependent on seasonal changes in the availability of new substrate produced by photosynthesis (Reichstein & Beer, 2008). Building on this idea, Migliavacca *et al.* (2011) showed that a significant improvement in the skill of a semiempirical R_{ECO} model (TPLinGPP) could be obtained by including GPP, along with temperature and water availability, as an additional driver. However, TPLinGPP underestimates R_{ECO} during the spring green-up (Fig. 1a and c) in deciduous forests (Migliavacca *et al.*, 2011).

Here, we investigate the hypothesis that the bias in spring green-up is related to a peak in autotrophic respiration resulting from the intense metabolic activity during the leaf out, which was not accounted for in the TPLinGPP model. This phenomenon of seasonal changes in plant physiology is referred as 'physiological phenology', which extends the traditional organism-focused definition of phenology to include physiological processes (Lieth, 1974). Here, we quantify physiological phenology in terms of the first derivative of a dynamic indicator of the state of the canopy. As indicators we use GPP and the fraction of Absorbed Photosynthetically Active Radiation (fAPAR).

The rate of aboveground autotrophic respiration is influenced by foliar development because the most immediate interactions between respiration and photosynthesis occur inside the leaves (Amthor, 1994b). Therefore, the phenology of foliar respiration typically tracks the phenology of photosynthesis (Amthor, 1994a; Ludwig *et al.*, 1994; Law *et al.*, 1999), except during spring green-up, when a large fraction of foliar respiration results from respiration costs associated with the construction of new leaves. Studies on several species showed that the costs of expanding buds during this period of high carbon demand are supported by carbohydrate reserves in woody tissues, rather than by

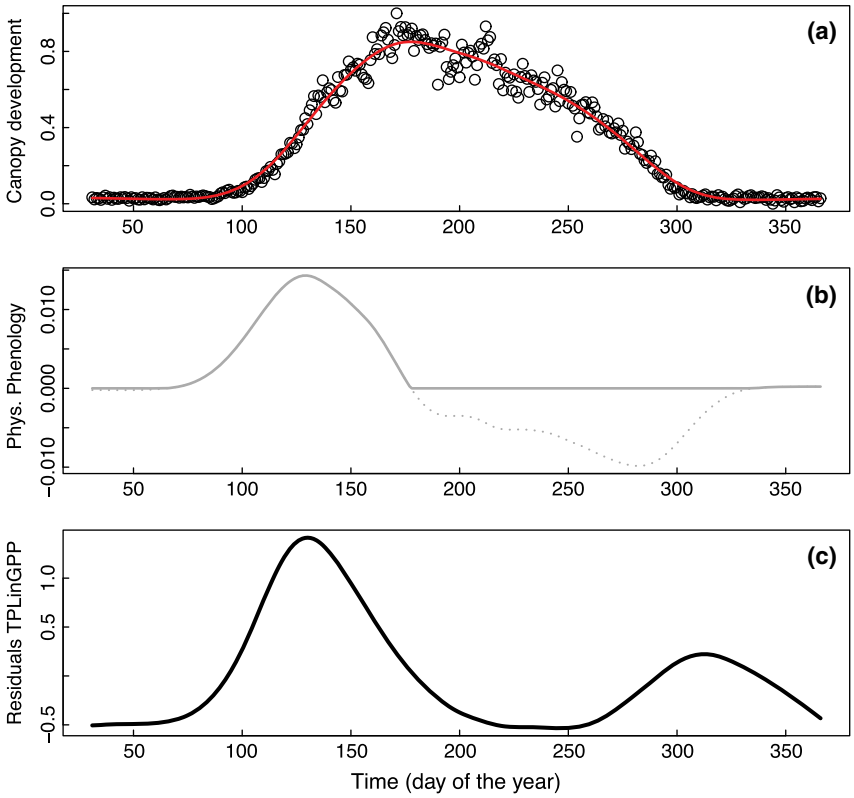

Fig. 1 Schematic representation of the processes. (a) Daily gross primary production (GPP) (the red line is a smoothed GPP). (b) First derivative of smoothed GPP (physiological phenology). (c) Example of model residuals of the TPLinGPP.

photosynthetic tissue (Landhäusser, 2010; Dickmann & Kozlowski 1970). The phenology of stem respiration is synchronous to wood production which, in turn, is determined by photosynthesis (Sprugel *et al*., 1995; Edwards & Hanson, 1996) and temperature. The stem respiration sensitivity to temperature varies from species to species and depends on the temperature to which plants are adapted or acclimated (Korner & Larcher, 1988). Moreover, a distinct pulse in stem respiration during the spring green-up has been observed in few studies (e.g., Bolstad *et al*., 2004).

The influence of physiological phenology on belowground autotrophic respiration has been reported in the literature as well. Joslin *et al.* (2001) found a correlation between a phenology index and root elongation intensity (Wilson & Batchelard, 1975) in a mature white oak-chestnut/oak forest in Tennessee (USA). Joslin *et al.* (2001) further showed that factors related to phenology appeared to override environmental variables such as soil water content in controlling the root elongation rate. To explain the results, the authors referred to Hendrick & Pregitzer (1996), who showed a burst of fine root growth in early summer immediately following foliar expansion, when soil water content and temperature conditions are favorable and the supply of carbohydrates produced by the newly expanded canopy is adequate. In fact, an increasing contribution of the autotrophic root respiration to soil respiration has been observed during the spring period of root elongation and growth (Law *et al*., 2001; Misson *et al*., 2006). Other studies reported even greater increases (30–50%) in the contribution of autotrophic respiration to total soil respiration during the growing season for different temperate deciduous forests (Epron *et al*., 2001). Physiological phenology has been shown to control belowground respiration also through the supply of photosynthates for the respiration of roots, mycorrhiza, and heterotrophs utilizing root exudates in the rhizosphere (CurielYuste *et al*., 2004; DeForest *et al*., 2006; Davidson & Holbrook, 2009). Recently, additional insights on the seasonality of carbon cycling processes were provided by studies using radiocarbon (^{14}C) signatures (Carbone *et al*., 2011). For example, Atarashi-Andoh *et al.* (2012) partitioned soil respiration into heterotrophic and autotrophic components using ^{14}C signatures and an isotope mass balance approach. They found that the contribution of root-derived carbon to soil respiration in a cool-temperate deciduous forest varied according to vegetation phenology.

Because respiratory fluxes are generated by different ecosystem components, the temperature driving respiration processes might varies according to: (i) the location where they take place, and (ii) the relative importance of the aboveground (primarily driven by air temperature, T_A) to belowground (primarily driven by soil temperature, T_S) components (e.g., Subke & Bahn, 2010;. Therefore, the analysis of the differences and biases introduced by the choice of the driving temperature in modeling respiration is increasingly studied (e.g., Richardson *et al*., 2006; Lasslop *et al*., 2012).

The overarching objective of this study is to improve the prediction of R_{ECO} of deciduous forests during spring green-up as compared to the work of Migliavacca *et al.* (2011) by including a representation of physiological phenology into the TPLinGPP model. To this end we: (i) developed a modified version of TPLinGPP that includes one of two alternative proxies of physiological phenology, (ii) optimized the modified model against R_{ECO} data reported for 19 deciduous forest eddy covariance sites, (iii) analyzed the reduction of model-data bias arising from the use of physiological phenology, and (iv) evaluated model performance using alternatively soil and air temperature as drivers of respiration with the aim of quantifying the relative importance of the belowground *vs*. aboveground respiration components during the season.

Material and methods

The dataset

In this analysis, data from version 2 of the LaThuile FLUXNET dataset (http://www.fluxdata.org) were used. The LaThuile dataset contains 253 research sites belonging to the FLUXNET eddy covariance flux measurements network (Baldocchi, 2008). The analysis focused on 19 deciduous broadleaved forest sites (Table 1) that have at least 1 year of good quality CO_2 fluxes and meteorological data (i.e., only days with <15% of gap-filled half-hours were retained), and maximum leaf area index (LAI) (Migliavacca *et al*., 2011).

These sites are located in the Northern Hemisphere in a latitudinal range that spans from 63.92°N at the Bonanza Creek site (US-Bn2) to 38.74°N at the Missouri Ozark site (US-MOz). The climatic regions analyzed include Humid Mesothermal Climates to Humid Microthermal Climates (classes C and D), according to the Köppen classification (Peel *et al*., 2007).

The following daily data products of the FLUXNET dataset were used: R_{ECO}, GPP, midday net ecosystem exchange (NEE) (11:00–13:00 hours), nighttime NEE [average of half-hourly NEE selected according to a global radiation threshold of 20 Wm^{-2} as defined by Reichstein *et al*. (2005)], daily mean air temperature (T_A), soil temperature (T_S), and 30-day backward precipitation running average (P). At each site, flux data were storage-corrected and spike-filtered as described in Papale *et al.* (2006), and subsequently gap-filled and partitioned as described by Reichstein *et al.* (2005).

For each site, we used estimates of fAPAR, retrieved from the Sea-viewing Wide Field-of-view Sensor (SeaWiFS) following methods of Gobron *et al.* (2000). The validation of the Joint Research Centre (JRC) fAPAR products (hereafter referred as

Table 1 List of deciduous broadleaf sites used in the analysis

Site ID	Tower Name	Country	Latitude	Longitude	Climate	References
CA-Oas	Sask. – SSA Old Aspen	Canada	53.63	−106.20	Dfc	(Black *et al.* 2000)
DE-Hai	Hainich	Germany	51.08	10.45	Cfb	(Knohl *et al.*, 2003)
FR-Fon	Fontainebleau	France	48.48	2.78	Cfb	(Delpierre *et al.*, 2009)
FR-Hes	Hesse Forest – Sarrebourg	France	48.67	7.06	Cfb	(Granier *et al.*, 2000)
IT-LMa	La Mandria	Italy	45.15	7.58	Cfa	(Reichstein *et al.*, 2005)
IT-Non	Nonantola	Italy	44.69	11.09	Cfa	(Reichstein *et al.*, 2005)
IT-PT1	Zerbolò–Parco Ticino– Canarazzo	Italy	45.20	9.06	Cfa	(Migliavacca *et al.*, 2009)
IT-Ro1	Roccarespampani 1	Italy	42.41	11.93	Csa	(Reichstein *et al.*, 2003)
IT-Ro2	Roccarespampani 2	Italy	42.39	11.92	Csa	(Reichstein *et al.*, 2003)
UK-Ham	Hampshire	UK	51.15	−0.86	Cfb	–
US-Bar	Bartlett Experimental Forest	USA	44.06	−71.29	Dfb	(Jenkins *et al.*, 2007)
US-Bn2	Bonanza Creek, 1987 Burn site	USA	63.92	−145.38	Dsc	(Liu *et al.*, 2005)
US-Ha1	Harvard Forest EMS Tower (HFR1)	USA	42.54	−72.17	Dfb	(Urbanski *et al.* 2007)
US-LPH	Little Prospect Hill	USA	42.54	−72.18	Dfb	(Borken *et al.*, 2006)
US-MMS	Morgan Monroe State Forest	USA	39.32	−86.41	Cfa	(Schmid *et al.*, 2000)
US-MOz	Missouri Ozark Site	USA	38.74	−92.20	Cfa	(Gu *et al.*, 2006)
US-Oho	Oak Openings	USA	41.55	−83.84	Dfa	(DeForest *et al.*, 2006)
US-UMB	University of Michigan Biological Station	USA	45.56	−84.71	Dfb	(Gough *et al.*, 2008)
US-WCr	Willow Creek	USA	45.81	−90.08	Dfb	(Cook *et al.*, 2004)

JRC fAPAR) is described by Gobron *et al.* (2006). The fAPAR used in this study covers the period from September 1997 to June 2006 with a nominal spatial resolution of 1.5 km (http://fAPAR.jrc.ec.europa.eu/) (Gobron *et al.*, 2006). The fAPAR values correspond to the 10-day time composite products spatially averaged over 3 × 3 pixels around the tower location. For the analysis of the spatial heterogeneity of the canopy fAPAR standard spatial deviations were classified into low, medium, and high variability according to the terciles of the distributions of the spatial standard deviation of the fAPAR.

Ecosystem respiration model

Description of TPLinGPP model. The semiempirical ecosystem respiration model, TPLinGPP [Eqn (1)], was based on the TP Model, a climate-driven model proposed by Raich *et al.* (2002), and further modified by Reichstein *et al.* (2003) and cross-validated by using R_{ECO} estimates from the FLUXNET network (Migliavacca *et al.*, 2011). The TPLinGPP concept was developed to simulate R_{ECO} as a function of daily ambient temperature T (which, if not declared otherwise is usually, T_A), P, and some base respiration rate as:

$$R_{ECO} = R_{ref} \cdot f(T) \cdot g(P), \quad (1)$$

where R_{ref} ($gCm^{-2}\ day^{-1}$) is the base ecosystem respiration (i.e., R_{ECO}) at the reference temperature (T_{ref}, K) without water limitations and is expressed as follows:

$$R_{ref} = R_0 + h(GPP), \quad (2)$$

where R_0 is the theoretical ecosystem respiration at T_{ref} when no other limiting factor interferes. R_0 can be considered to be a functional indicator of site ecosystem respiration, closely related to structural site characteristics (e.g., LAI) and history (e.g., management and disturbance, Migliavacca *et al.*, 2011). The term h(GPP) represents the dependency of reference respiration on productivity:

$$h(GPP) = k_2 \cdot GPP, \quad (3)$$

where k_2 represents the influence of supply via GPP on R_{ref}. The temperature dependence of R_{ECO} is modeled by using an Arrhenius-type equation:

$$f(T_A) = e^{E_0 \cdot \left(\frac{1}{T_{ref}-T_0} - \frac{1}{T-T_0}\right)} \quad (4)$$

E_0 (K) is the activation energy parameter and represents the sensitivity of ecosystem respiration to temperature, T_{ref} is fixed here at 288.15 K (15 °C) and T_0 is fixed at 227.13 K (−46.02 °C) (Lloyd & Taylor, 1994).

The response of R_{ECO} to precipitation was formulated as a function of P, the 30-day backward running average of precipitation:

$$g(P) = \frac{\alpha \cdot k + P(1-\alpha)}{k + P(1-\alpha)} \quad (5)$$

where k (mm) is the half saturation constant of the hyperbolic relationship and α is the response of R_{ECO} to zero P. Soil water content is widely recognized as a viable descriptor of soil water availability, and the use of precipitation can be limiting for the simulation of R_{ECO} in forest sites where precipitation and soil water content are not tightly coupled. However, we preferred to use precipitation since the model was developed with an emphasis toward upscaling to larger areas and soil water maps have greater uncertainty than precipitation distributions (Peters-Lidard *et al.*, 2008), and are often difficult to obtain. On the other hand, satellite remote sensing data only capture the very first centimeters of the soil and are, therefore, only partly representative for the available water for plants.

Development of the TPdGPP model. TPLinGPP was modified in the present study to reduce the spring bias observed over deciduous forests. A key insight from previous studies is that R_{ref} can be assumed to vary during the growing season, but is dependent of specific site characteristics (Reichstein *et al*., 2003; Migliavacca *et al*., 2011), productivity (GPP, Mahecha *et al*., 2010a; Migliavacca *et al*., 2011), and physiological phenology.

The first derivative of a canopy development indicator in spring was introduced to reduce the spring bias in modeled R_{ECO}. Specifically, either GPP or fAPAR was used for this purpose, and the daily values of the first derivative of their smoothed time series (i.e., dGPP/dt and dfAPAR/dt, respectively) were computed. For this purpose the time series of daily GPP and 10-daily fAPAR were smoothed and gap-filled using a cubic spline with degrees of freedom adjusted to the length of the time series (30 for GPP and 20 for fAPAR). The first derivatives were numerically computed from the smoothed time series. Because our focus is on the spring period, we set the negative values of the first derivative that occurred in autumn to 0, retaining only values of dGPP/dt>0 (Fig. 1b).

The TPLinGPP was then modified by introducing the sensitivity to reference respiration to dGPP/dt (or dfAPAR/dt) as follows:

$$R_{ref} = R_0 + h(\mathrm{GPP}) + i\left(\frac{\mathrm{dGPP}}{\mathrm{dt}}\right) \quad (6)$$

The final TPdGPP equation is:

$$R_{ECO} = \left(R_0 + k_2\mathrm{GPP} + k_{20}\cdot\frac{\mathrm{dGPP}}{\mathrm{dt}}\right)\cdot e^{E_0\cdot\left(\frac{1}{T_{ref}-T_0}-\frac{1}{T-T_0}\right)} \cdot\frac{\alpha\cdot k + P(1-\alpha)}{k + P(1-\alpha)} \quad (7)$$

where k_{20} is the parameter describing the linear dependency of the reference respiration to physiological phenology (dGPP/dt or dfAPAR/dt).

Modeling set-up. The parameters in TPLinGPP [R_0, E_0, α, k, and k_2 in Eqns (1–5)] and in TPdGPP [R_0, E_0, α, k, k_2, and k_{20}, in Eqn (7)] were estimated for each site.

An initial analysis was conducted using the following combination of driver-observations: daily GPP, the first derivative of midday GPP, and R_{ECO} reported in the FLUXNET database (hereafter, we refer to this driver-observation set with the label GPP-dGPP-R_{ECO}). The parameters of the TPdGPP model were estimated using alternatively soil (T_S) and air (T_A) temperature. Then, with a moving window of 2 weeks, we computed the ratio of the coefficient of determination (R^2) of the TPdGPP model simulations driven by T_S to that driven by T_A. The latter analysis was conducted to evaluate the ability of T_S and T_A in predicting R_{ECO}. When the ratio was lower than 1, a relevant contribution of aboveground respiration to the temporal variability of R_{ECO} can be hypothesized.

A second exercise was conducted using nighttime NEE in place of R_{ECO}, midday NEE (11:00–13:00 hours) in place of GPP and dfAPAR/dt as a proxy for canopy development. This analysis was conducted to confirm the results obtained with the first analysis, because GPP and R_{ECO} are partially correlated. Hereafter, we refer to this driver-observation set with the label NEEm-dfAPAR-NEEn (Table 2).

Finally, with the aim of detecting possible time-lags between respiration response and the peak of dGPP/dt, we ran the model with different time lagged dGPP/dt time series, starting from the dGPP/dt estimated on the same day up to a maximum lag time of 10 days after the measured R_{ECO}. The springtime peak of the rate of R_{ECO} might precede the dGPP/dt peak because the production of new leaves requires an increase of metabolic activity (e.g., translocation of carbon stored in woody tissues) that might precede the start of the carbon uptake period and the increase of GPP.

Statistical analysis

Estimation of model parameters and evaluation of model performance. Model parameters were estimated using the Levenberg–Marquardt method, implemented using the *optim* routine in R (version 2.14.0). Model parameter standard errors were estimated based on 500 bootstrap samples. As described by Efron & Tibshirani (1993), the obtained distribution of parameter estimates approximates the distribution of the 'true' model parameters.

Table 2 Summary of the model runs conducted and drivers

	TPdGPP		TPLinGPP	
	GPP-dGPP-R_{ECO}	NEEm-dfAPAR-NEEn	GPP-dGPP-R_{ECO}	NEEm-dfAPAR-NEEn
Drivers				
Daily GPP	■		■	
Daily midday NEE		■		■
Daily first derivative GPP	■			
Daily first derivative fAPAR		■		■
Daily Temperature	■	■	■	■
30-day running average P	■	■	■	■
Constrains				
Daily R_{ECO}	■		■	
Daily night-time NEE		■		■

Model performance was evaluated using a range of metrics (root mean square error, RMSE; coefficient of determination, R^2; and mean absolute error, MAE; Janssen & Heuberger, 1995) to examine whether the inclusion of physiological phenology improved the description of the temporal variability of R_{ECO}. Modeling efficiency (EF), a measure of the coincidence between observed and modeled data, was also computed. EF ranges between -∞ to 1. A value of 1 corresponds to a perfect match between model and observation, while EF <0 indicate that the mean of the observations is a better predictor than the model. EF is sensitive to systematic deviation between model and observation (Janssen & Heuberger, 1995). Model statistics and residuals (observation-modeled value) were computed for the whole year and for each season (MAM, March–April–May; JJA, June–July–August; SON, September–October–November; and DJF, December–January–February) in order to evaluate the improvement in the description of the seasonal cycle of R_{ECO}.

The Akaike's Information Criterion (AIC) was used to select amongst the two alternative model formulations considering both model explanatory power and the model complexity (i.e., number of parameters). The following formulation was used (Anderson *et al.*, 2000; Richardson *et al.*, 2006):

$$\mathrm{AIC} = 2(p+1) + n\log(\hat{\sigma}^2), \quad (8)$$

where n is the number of observations (i.e., days in the time series), $\hat{\sigma}^2$ equals the estimated within-sample residual sum of squares divided by n, and p is the number of parameters in the model. The model with the lowest AIC was considered the best model. The differences between the AIC (ΔAIC) computed for the TPdGPP ($\mathrm{AIC_{TPdGPP}}$) model and the TPLinGPP ($\mathrm{AIC_{TPLinGPP}}$) were computed. Negative differences indicated that the TPdGPP model, despite the higher complexity, was the best model formulation for the target dataset.

Spectral analysis of model residuals. Singular spectral analysis (SSA, Golyandina *et al.*, 2001) was used to analyze periodicities in the residuals of TPLinGPP and TPdGPP, and to verify whether the seasonal bias in R_{ECO} decreased by including GPP development rate as an additional driver. The analysis was conducted both for the driver-observation set GPP-dGPP-R_{ECO} and NEEm-dfAPAR-NEEn.

The idea behind SSA is that each observed time series is a set of (linearly) superimposed subsignals (Golyandina *et al.*, 2001). Partitioning a time series into subsignals can be used to separate the slow (multi-year) signals from the annual cycle and higher frequency components. SSA allows for the extraction of amplitude- and phase-modulated subsignals from the original time series and, hence, enables the analyst to investigate processes at multiple time scales. Mahecha *et al.* (2007) showed that SSA can be used to extract components of ecosystem fluxes corresponding to specific time scales that might be useful for improved process understanding (Mahecha *et al.*, 2010a) and model evaluation (Mahecha *et al.*, 2010b). We conducted our SSA analysis as follows:

1 Because only days with <15% of gap-filled half-hours were retained, the time series of daily GPP and R_{ECO} contain gaps. We filled the gaps in the time series with an inherent SSA gap-filling strategy (Kondrashov & Ghil, 2006), as spectral analyses generally require gap-free records, whenever the FLUXNET methodology did not provide accurate estimates.
2 The annual and monthly subsignals were extracted at each site from the observed R_{ECO} and the simulated series resulted from different model structures (TPLinGPP, TPdGPP).
3 We retained only the original points (i.e., days not gap-filled during the step 1) from decomposed time series and computed the model-observation residuals of the different components of the time series (i.e., annual-seasonal, monthly).
4 The variance of residuals from each component was computed for each time scale. The time-explicit decomposition allows for localizing mismatches between observations and models in frequency class and in time. This is a substantial advantage compared to conventional spectral analyses.

The annual-seasonal bins are defined here by periods in the interval (330:400) days (hereafter referred to as annual time scale), while the monthly component is defined by periods in the interval (30:60) days (hereafter referred to as monthly time scale).

Results

Evaluation of models performance

Across sites, the mean EF obtained for the two models, using the driver-observations GPP-dGPP-R_{ECO}, was 0.72 [interquartile distance 0.64–0.82] for the TPLinGPP model, and 0.76 [0.68–0.83] for the TPdGPP model (Table 3). For the driver-observations NEEm-dfAPAR-NEEn, the mean EF decreased to 0.66 (0.70) for the TPLinGPP (TPdGPP) (Table 4). By using the explicit description of physiological phenology, a decrease in RMSE of ~8% was achieved for GPP-dGPP-R_{ECO} and ~3% for NEEm-dfAPAR-NEEn. The largest improvement of model performance was observed at DE-Hai, FR-Fon, US-Bn2, IT-LMa, IT-Ro2, and US-MOz. Almost no improvement in model performance was observed at CA-Oas, FR-Hes, US-UMB, and US-LPH. The mean ΔAIC of −91.11 (−31.14) obtained for the driver-observations GPP-dGPP-R_{ECO} (NEEm-dfAPAR-NEEn) indicated that, even accounting for the higher models complexity (i.e., 1 parameter more), the TPdGPP model outperforms the TPLinGPP (Tables 3 and 4).

The use of the TPdGPP model led to a reduction of the model-observation mismatch, particularly in spring (Figs 2,3, Table 5). The reduction of annual model residuals was not as relevant as that at seasonal time scale, likely because the seasonal bias in spring was partly compensated by negative biases in summer.

Spectral analysis of model residuals

The boxplots of the model residual variance computed at each site for the monthly and annual time scales indicated a tendency toward lower variance on the monthly time scale for the TPdGPP model compared to the TPLinGPP model, for both driver-observation combinations (Fig. 4). On the annual time scale, a reduction in residual variance was also observed, however, differences were less pronounced than at the monthly time scale. For the driver-observations NEEm-dfAPAR-NEEn, the reduction of the residual variance at the monthly time scale was lower at sites with high spatial heterogeneity (Fig. 5). The latter was derived using the spatial standard deviation of JRC fAPAR computed in spring (Fig. 5a) and during the whole year (Fig. 5b).

Sources of uncertainty for the TPdGPP model

Comparing R^2 values for the TPdGPP model driven by T_S and T_A indicates that the model driven by T_A outperformed the model driven by T_S in winter and early spring, while the R^2 are similar in August and September (Fig. 6). The relative differences in RMSE between the TPLinGPP and TPdGPP model driven by T_S and T_A were generally low, except in a few sites (CA-Oas, IT-PT1, US-LPH, US-MMS, US-UMB; Table 6). At these sites we observed a small improvement of the performance using the TPdGPP model driven by T_A, whereas, when using T_S, the reduction of RMSE was larger, indicating that T_S is likely the most important driver over these sites. The analysis conducted with a lagged response between dGPP/dt and R_{ECO} did not show a clear relationship between improvement in model performance and the time lag. Only the two sites with the largest improvement in model performances (i.e., DE-Hai and FR-Fon) were characterized by no or short lags between the physiological phenology and R_{ECO}, whereas at sites with a larger lag time, the improvement in model performance from introducing TPdGPP was less important (Fig. 7).

Discussion

Physiological phenology controls on ecosystem respiration

In a previous study, (Migliavacca *et al.*, 2011) we showed that taking into consideration the dependency

Table 3 Performance statistics (root mean square error, RMSE, and modeling efficiency, EF) of the TPLinGPP model and the model including the explicit description of physiological phenology (TPdGPP). Data are obtained by fitting the model to the ecosystem respiration data and using as forcing the gross primary productivity and its first derivative. ΔAIC represents the differences between the AIC computed for the TPdGPP (AIC_{TPdGPP}) model and the TPLinGPP ($AIC_{TPLinGPP}$). Negative differences indicate that the TPdGPP model outperforms the TPLinGPP model. *n* represents the number of data values used for the analysis

	TPdGPP		TPLinGPP			
Site	RMSE ($gC\ m^{-2}\ day^{-1}$)	EF	RMSE ($gC\ m^{-2}\ day^{-1}$)	EF	ΔAIC	*n*
CA-Oas	0.65	0.92	0.65	0.92	2.0	2914
DE-Hai	0.60	0.84	0.83	0.70	−525.9	1873
FR-Fon	0.78	0.82	1.00	0.71	−132.6	593
FR-Hes	1.49	0.63	1.49	0.63	2.0	3132
IT-LMa	0.67	0.73	0.74	0.67	−41.8	507
IT-Non	0.81	0.80	0.81	0.80	2.0	794
IT-PT1	0.77	0.83	0.78	0.82	2.0	802
IT-Ro1	0.95	0.61	1.01	0.56	−81.5	1895
IT-Ro2	0.68	0.68	0.77	0.58	−525.9	1170
UK-Ham	1.16	0.68	1.29	0.60	−50.04	564
US-Bar	0.85	0.67	0.89	0.64	−16.61	466
US-Bn2	0.34	0.90	0.37	0.89	−61.7	212
US-Ha1	0.91	0.74	0.98	0.71	−19.1	2358
US-LPH	1.29	0.53	1.30	0.53	−25.4	440
US-MMS	0.65	0.83	0.66	0.83	−56.2	2064
US-MOz	0.81	0.86	0.88	0.83	−5.0	808
US-Oho	0.91	0.71	0.93	0.70	−17.5	373
US-UMB	0.65	0.90	0.69	0.89	−166.2	1537
US-WCr	1.68	0.78	1.75	0.76	−13.6	1784
Mean	0.87	0.76	0.96	0.72	−91.11	
(0.25–0.75)	(0.65–0.95)	(0.68–0.83)	(0.76–1.08)	(0.64–0.82)	(−71.6–9.3)	

Table 4 Performance statistics (Root Mean Squared Error, RMSE, and modeling efficiency, EF) of the TPLinGPP model and the model including the explicit description of physiological phenology (TPdGPP). Data are obtained fitting the model against night-time net ecosystem exchange data and using as forcing the midday net ecosystem exchange and the first derivative of the fraction of absorbed photosynthetic radiation. ΔAIC represents the differences between the AIC computed for the TPdGPP (AIC_{TPdGPP}) model and the TPLinGPP ($AIC_{TPLinGPP}$). Negative differences indicate that the TPdGPP model outperforms the TPLinGPP model. *n* represents the number of data used for the analysis

	TPdGPP		TPLinGPP			
Site	RMSE ($gC\ m^{-2}\ day^{-1}$)	EF	RMSE ($gC\ m^{-2}\ day^{-1}$)	EF	ΔAIC	*n*
CA-Oas	0.73	0.90	0.74	0.90	−32.44	2914
DE-Hai	0.74	0.76	0.88	0.66	−279.89	1873
FR-Fon	1.19	0.58	1.20	0.57	−2.31	593
FR-Hes	1.72	0.51	1.72	0.51	2.00	3132
IT-LMa	0.84	0.58	0.85	0.57	−3.21	507
IT-Non	1.10	0.63	1.12	0.62	−10.43	794
IT-PT1	0.8	0.81	0.80	0.81	2.00	802
IT-Ro1	1.06	0.52	1.16	0.42	−146.39	1895
IT-Ro2	0.68	0.68	0.77	0.58	−3.21	1170
UK-Ham	1.16	0.68	1.29	0.60	−50.04	564
US-Bar	0.85	0.67	0.89	0.64	−16.61	466
US-Bn2	0.36	0.89	0.46	0.82	−43.14	212
US-Ha1	1.04	0.67	1.03	0.67	21.79	2358
US-LPH	1.28	0.54	1.28	0.54	2.00	440
US-MMS	0.70	0.80	0.70	0.80	2.00	2064
US-MOz	1.00	0.78	1.01	0.78	−4.98	808
US-Oho	1.06	0.61	1.12	0.56	−15.84	373
US-UMB	0.78	0.86	0.79	0.86	−15.01	1537
US-WCr	2.10	0.66	2.10	0.66	2.00	1784
Mean	1.04	0.70	1.07	0.66	−31.14	
(0.25–0.75)	(0.36–2.1)	(0.51–0.89)	(0.46–2.1)	(0.42–0.86)	(−24.53–2.0)	

Table 5 Average of the daily model residuals ($g\ Cm^{-2}$)at each site computed over different seasons. TPlinGPP model is the model driven by climate and productivity. TPdPP is the model driven by climate, productivity, and physiological phenology. GPP-dGPP-R_{ECO} denotes models fitted against ecosystem respiration and driven by gross primary productivity (GPP) and its first derivative. NEEm-dfAPAR-NEEn denotes models fitted against night-time net ecosystem exchange (NEEn) and driven by midday NEE and the first derivative of the fraction of absorbed photosynthetic radiation (fAPAR)

	GPP-dGPP-R_{ECO}		NEEm-dfAPAR-NEEn	
Period	TPdGPP	TPLinGPP	TPdGPP	TPLinGPP
DJF	−0.08 (0.80)	−0.11 (0.79)	−0.05 (0.80)	−0.09 (0.79)
MAM	−3.91 (0.90)	7.82 (0.87)	0.39 (0.84)	0.44 (0.79)
JJA	−2.99 (0.87)	−7.19 (0.87)	0.82 (0.80)	0.83 (0.79)
SON	0.17 (0.83)	0.10 (0.82)	0.29 (0.79)	0.27 (0.80)
Year	2.12 (0.91)	4.31 (0.90)	0.41 (0.86)	0.42 (0.84)

of R_{ECO} on some measure of short-term productivity (e.g., via coupling the base respiration to GPP) improved the skill of empirical R_{ECO} models significantly. Here, we show that, for a sample of deciduous broadleaved forests, R_{ECO} is controlled by climate (temperature and precipitation pulses) and canopy photosynthesis, and also by springtime physiological phenology. The latter can be approximated by the first derivative of daily smoothed GPP or fAPAR. The results obtained with the combination GPP-dGPP-R_{ECO} were more robust than those obtained with NEEm-dfAPAR-NEEn. This might be due to the higher noise in NEE time series, to scale mismatch between the eddy covariance flux tower and satellite footprint (Jung *et al.*, 2008), and to the fact that nighttime NEEn reflects primarily the dynamics of soil respiration and, to a lesser extent, the dynamics of the aboveground respiration that are an important cause for the bias observed during the springtime period. Fig. 5 highlights that the largest reduction of the model-observation bias was observed in spatially homogeneous sites, suggesting that the proposed approach is sensitive to landscape heterogeneity. GPP is a more direct descriptor of the canopy photosynthetic capacity than fAPAR, which tracks the development of leaf area index. Interestingly, regardless of the driver-observations used (i.e., NEEm-dfAPAR-NEEn and GPP-dGPP-R_{ECO}), we identified a

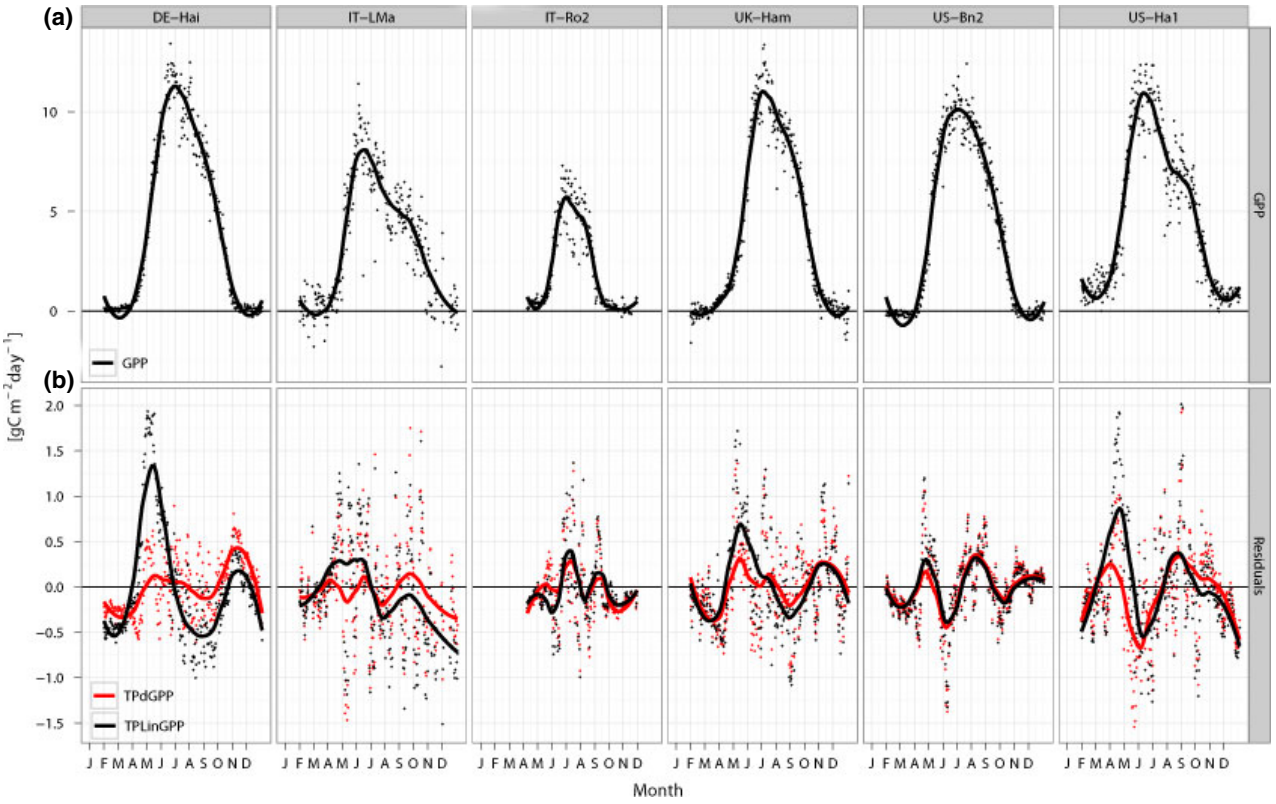

Fig. 2 Mean seasonal variation of daily gross primary production (GPP) and smoothed GPP (a), model residuals of TPLinGPP (black line) and TPdGPP (red line) (b) and the respective color dots. Data from a subsample of sites.

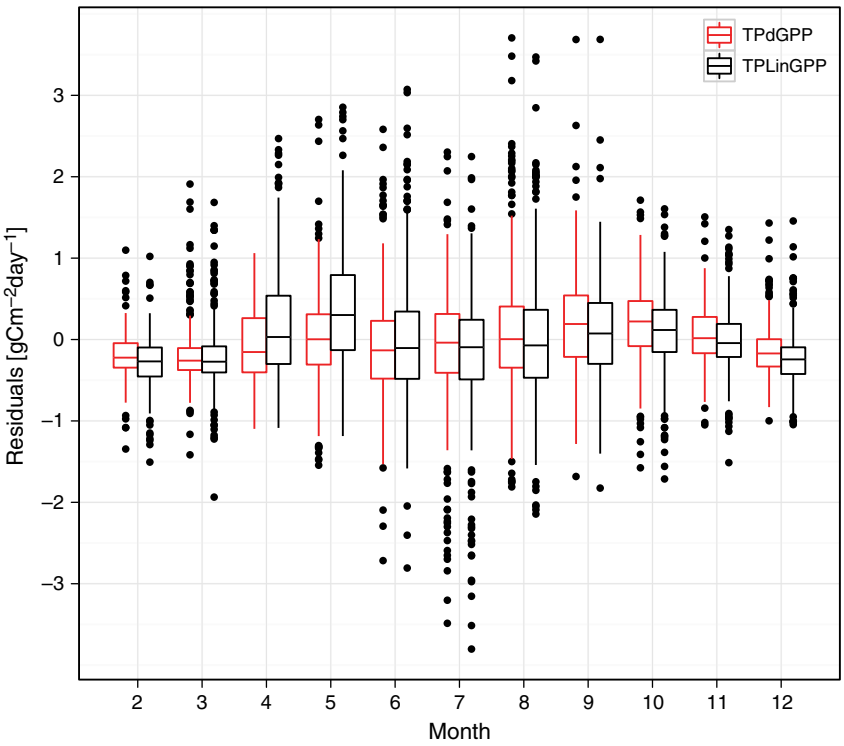

Fig. 3 Mean seasonal variation of daily model residuals: TPLinGPP in black boxes and TPdGPP in red boxes.

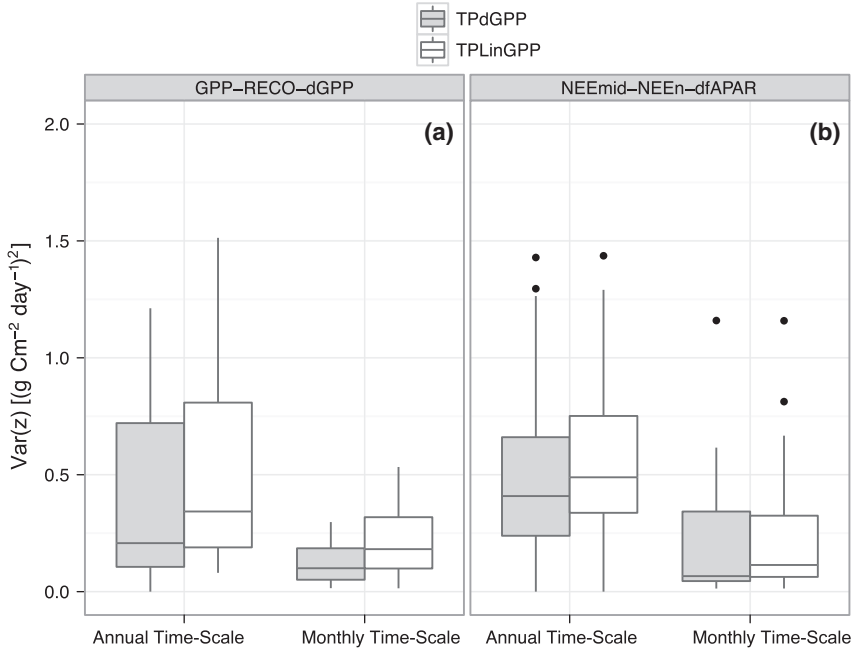

Fig. 4 Boxplot of the variance of residuals at monthly and annual time scale. Gray boxes represent residuals of TPdGPP and white boxes represent residuals of TPLinGPP. The panel (a) represents results obtained with the combination of driver-observation GPP-dGPP-R_{ECO} while (b) results obtained with NEEm-dfAPAR-NEEn.

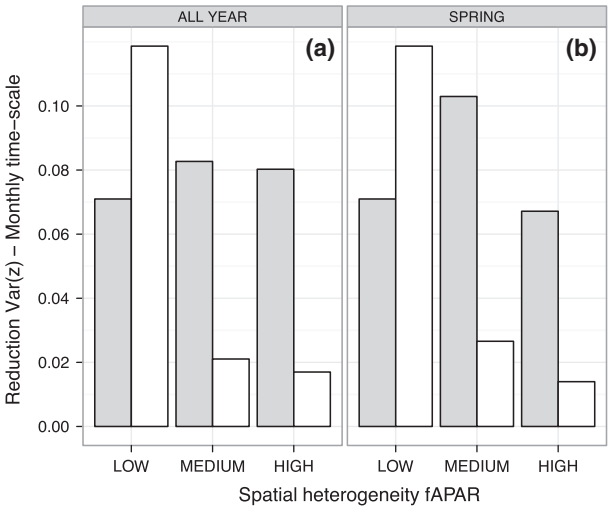

Fig. 5 Reduction of the variance of residuals in classes of spatial heterogeneity for the all year (a) and for spring (b). Gray histograms represent the results obtained with the driver-observation set GPP-dGPP-R_{ECO} while white histograms represents the driver-observation set NEEm-dfAPAR-NEEn.

clear effect of physiological phenology on R_{ECO}. This finding leads to the proposed data-oriented semiempirical model that takes these linkages into account to improve the description of the seasonal cycle of R_{ECO}.

The analysis of the ratio of the R^2 between TPdGPP models driven by T_S and T_A confirms the importance of air temperature during springtime (Fig. 6), suggesting that aboveground respiration plays an important role in spring. This supports the need to include physiological phenology as an additional driver in modeling R_{ECO} (Irvine *et al.*, 2008). The seasonal dynamics observed in Fig. 6 are consistent with Davidson *et al.* (2006) and Giasson *et al.* (2013), who reported a spring pulse of aboveground respiration, leading to a minimum in the ratio between soil respiration and R_{ECO} in March and early April.

Limitations and future perspectives

Model performance statistics (Tables 3 and 4) show that the use of the explicit description of physiological phenology for some sites does not reduce the springtime bias in R_{ECO}. While all investigated sites are classified as deciduous broadleaved forests, some are composed of multiple tree species. Different species could have different and asynchronous phenological patterns that might confound the influence of physiological phenology on R_{ECO} at the ecosystem level. Moreover, considering that the R_{ECO} is observed at the ecosystem level with a variable footprint, the spatial heterogeneity of the canopy (Cescatti *et al.*, 2012) might contribute to the poor model performances at some sites. For sites characterized by no or short lags between the physiological phenology and R_{ECO}, TPdGPP showed the largest improvement, whereas for sites characterized by larger

Table 6 Differences in Root Mean Square Error (RMSE) between the TPLinGPP and TPdGPP at each site for runs conducted using air [$\Delta RMSE(T_A)$] and soil [$\Delta RMSE(T_S)$] temperature as driver

Site	$\Delta RMSE(T_A)$ (gC m^{-2} day^{-1})	$\Delta RMSE(T_S)$ (gC m^{-2} day^{-1})
CA-Oas	0.21	8.92
DE-Hai	27.42	30.30
FR-Fon	21.21	25.37
FR-Hes	2.39E-04	0.12
IT-LMa	9.38	12.03
IT-Non	0.26	5.81E-04
IT-PT1	0.76	5.58
IT-Ro1	6.16	6.61
IT-Ro2	14.30	14.85
US-Bar	5.57	9.05
US-Bn2	5.64	7.66
US-Ha1	3.94	3.26
US-LPH	0.19	1.17
US-MMS	0.73	5.18
US-MOz	6.40	6.64
US-Oho	2.01	1.80
US-UMB	0.96	7.12
US-WCr	4.35	6.51

lags the improvement of model performance by introducing TPdGPP was less (Fig. 7). For some sites, the springtime peak of R_{ECO} might precede the peak of dGPP/dt because production of new leaves requires an increase in metabolic activity (e.g., translocation of carbon stored in woody tissues) that would precede the onset of photosynthetic activity. This lag between foliage expansion and the development of photosynthetic capacity has been reported in the literature (e.g., Morecroft *et al.*, 2003) and might be one of the causes of the limited improvement in model performance for some sites.

Future work is necessary to reduce the autumn bias of R_{ECO}, though less pronounced than the bias in spring, observed with the empirical model proposed by Migliavacca *et al.* (2011). The autumn bias might be related to the rapid decomposition of fresh litter inputs (DeForest *et al.*, 2009), which is not accounted for by the empirical model. Decomposition in autumn may also be higher because of a large pulse of fine root turnover in addition to leaf litter fall. The inclusion of leaf or fine root litter pools would effectively turn our simple, empirical model into a more complex process-based model. Autumn bias might also be related to the

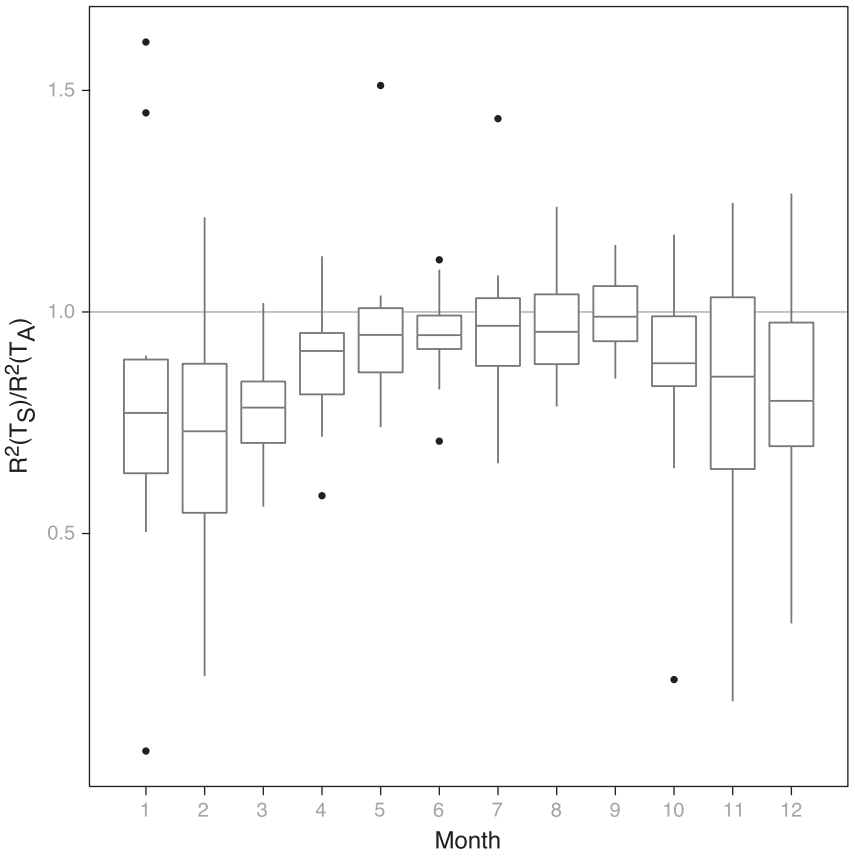

Fig. 6 Boxplot of the seasonal evolution of the ratio of the R^2 of TPdGPP driven by T_S to that driven by T_A. R^2 was computed for all sites with a sliding window.

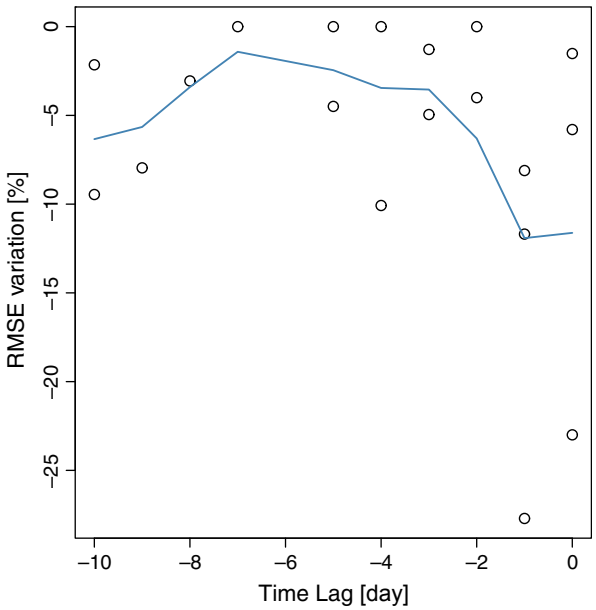

Fig. 7 Relationship between the relative difference of RMSE of TPLinGPP and TPdGPP model and the time lag between R_{ECO} and dGPP/dt maximizing the performance in fitting of the TPdGPP Model. Different points represent different sites.

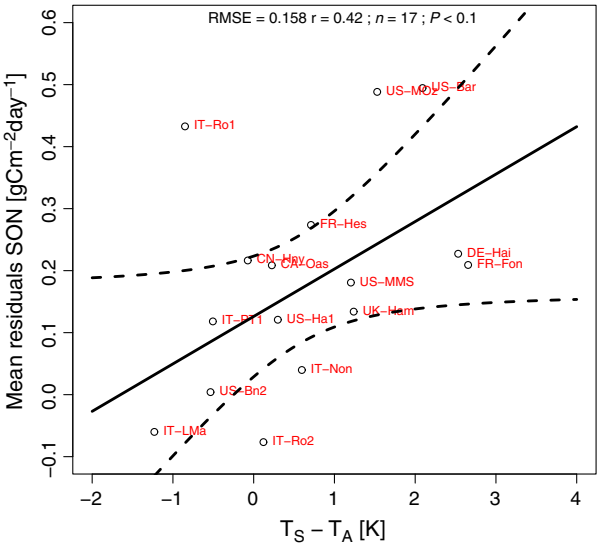

Fig. 8 Scatterplot between the mean difference of total residuals computed in autumn with the mean of the differences between soil temperature (T_S) and air temperature (T_A) in autumn. SON represents the period September–October–November. The correlation coefficient (r) is also reported.

difference between soil and air temperature, as soil temperature is higher than air temperature in the autumn. Thus, the TPLinGPP model driven by T_A may lead to an underestimation of autumn respiration. In Fig. 8, the mean residuals during autumn at each site are correlated ($r = 0.42$ $P < 0.1$) with the mean difference between daily mean autumn T_S and T_A. In general, sites with higher model residuals in autumn are the ones with a more positive soil–air temperature difference (i.e., soil warmer than air).

Implication for data-oriented modeling

DeForest *et al.* (2006) showed that phenophase-specific models of soil respiration improve estimates of annual respiration. In fact, incorporating phenology into soil respiration models indirectly accounts for changes in environmental and/or biological factors that were not explicitly defined in the proposed model. The authors suggested that, ideally, the component fluxes of respiration should be modeled independently, or at least grouped according to time windows and environmental conditions during which common regulatory mechanisms (e.g., phenology) can be assumed. In this study, we proposed an empirical model for R_{ECO} that includes the first derivative of GPP (or fAPAR) to explicitly account for the physiological phenology-related pulse of R_{ECO} during spring (from bud-break to leaf unfolding), before reaching the maximum LAI.

Our results suggest that the proposed model structure reduces the spring-summer bias in R_{ECO} estimates. Annual estimates of R_{ECO} are also less biased even though to a lesser extent than at seasonal time scale. This is probably due to the compensation of the model bias in spring (positive) and summer (negative) without the explicit dependency of R_{ECO} on physiological phenology. The spring bias is particularly relevant to global carbon cycle studies for several reasons. First, spring is considered the most critical period determining the interannual variability of the net ecosystem CO_2 uptake (Le Maire *et al.*, 2010) in ecosystems that are not characterized by summer drought and, therefore, an accurate modeling of respiration will likely improve estimates of the net CO_2 uptake in this crucial period. Second, the mean springtime and annual bias introduced by using the two different modeling approaches at global scale results in a difference in the net carbon uptake of about 1.4 PgC yr^{-1} at the annual time scale, while a difference of 0.6 PgC and 0.8 PgC are expected in spring and summer, respectively. These results were obtained by multiplying the average residuals by the global coverage of deciduous forests in m^2 [1752105 km^2 according to Hansen *et al.* (2000)]. The springtime bias in R_{ECO} might significantly affect the estimates of land–atmosphere CO_2 fluxes obtained from atmospheric inversion models when these data are used as priors. This is particularly relevant for regional-scale inversions because the distribution of temperate deciduous forests is divided mainly between Northern Eurasia and Northeastern America.

In conclusion, our study suggests that it is necessary to account for the dependence of ecosystem respiration on short-term productivity (e.g., daily GPP) and on the physiological phenology to guarantee reliable simulations of R_{ECO} of deciduous broadleaved forests. By explicitly including the effects of physiological phenology on R_{ECO}, we found that spring and summertime biases observed in previous studies are significantly reduced. This implies that for global or regional-scale application of data-oriented empirical models, some measure of rate of development of physiological phenology needs to be included to improve the simulation of seasonal and interannual variability of R_{ECO}. This improvement is necessary to strengthen the analysis and interpretation of the seasonal cycle of the global CO_2 growth rate and annual carbon balance. Although the present study using the FLUXNET database clearly reveals a tight linkage between physiological phenology and ecosystem respiration in deciduous forests, future experimental efforts should focus on refining the mechanistic understanding of this linkage. From a modeling perspective, future work is also needed to improve the simulation of the respiration pulse in autumn.

Acknowledgments

This work used eddy covariance data acquired by the FLUXNET community and in particular by the following networks: AmeriFlux (U.S. Department of Energy, Biological, and Environmental Research, Terrestrial Carbon Program (DE-FG02-04ER63917 and DE-FG02-04ER63911)), AfriFlux, AsiaFlux, CarboAfrica, CarboEuropeIP, CarboItaly, CarboMont, ChinaFlux, Fluxnet-Canada (supported by CFCAS, NSERC, BIOCAP, Environment Canada, and NRCan), GreenGrass, KoFlux, LBA, NECC, OzFlux, TCOS-Siberia, and the USCCC. We acknowledge the financial support to the eddy covariance data harmonization provided by CarboEuropeIP, FAO-GTOS-TCO, iLEAPS, Max Planck Institute for Biogeochemistry, National Science Foundation, University of Tuscia, Université Laval, Environment Canada and US Department of Energy and the database development and technical support from Berkeley Water Center, Lawrence Berkeley National Laboratory, Microsoft Research eScience, Oak Ridge National Laboratory, University of California – Berkeley and the University of Virginia, and the IceMe of NUIST. The authors would like to thank all the PIs of eddy covariance sites, technicians, postdoctoral fellows, research associates, and site collaborators involved in FLUXNET who are not included as coauthors of this paper, without whose work this analysis would not have been possible. ADR acknowledges support from the National Science Foundation, grants DEB-1114804 and EF-1065029. The authors thank Morgan Furze for editing the article for style and grammar, and the anonymous reviewers and the editor for the comments that improved the readability of the article.

References

Amthor JS (1994a) Plant respiratory responses to the environment and their effects on the carbon balance. In: *Plant-Environment Interactions* (ed. Wilkinson RE), pp. 501–554. Marcel Dekker, New York, NY, USA.

Amthor JS (1994b) Higher plant respiration and its relationships to photosynthesis. In: *Ecological Studies: Ecophysiology of Photosynthesis*, Vol **100** (eds Schultze E-D, Caldwell MM), pp. 71–101. Springer-Verlag, Berlin.

Anderson DR, Burnham KP, Thompson WL (2000) Null hypothesis testing: problems, prevalence, and an alternative. *Journal of Wildlife Management*, **64**, 912–923.

Atarashi-Andoh M, Koarashi J, Ishizuka S, Hirai K (2012) Seasonal patterns and control factors of CO2 effluxes from surface litter, soil organic carbon, and root-derived carbon estimated using radiocarbon signatures. *Agricultural and Forest Meteorology*, **152**, 149–158.

Baldocchi D (2008) TURNER REVIEW No. 15. 'Breathing' of the terrestrial biosphere: lessons learned from a global network of carbon dioxide flux measurement systems. *Australian Journal of Botany*, **56**, 1.

Black TA, Chen WJ, Barr AG *et al*. (2000) Increased carbon sequestration by a boreal deciduous forest in years with a warm spring. *Geophysical Research Letters*, **27**, 1271–1274.

Bolstad PV, Davis KJ, Martin J, Cook BD, Wang W (2004) Component and whole-system respiration fluxes in northern deciduous forests. *Tree Physiology*, **24**, 493–504.

Borken W, Savage K, Davidson EA, Trumbore SE (2006) Effects of experimental drought on soil respiration and radiocarbon efflux from a temperate forest soil. *Global Change Biology*, **112**, 177–193.

Carbone MS, Still CJ, Ambrose AR *et al*. (2011) Seasonal and episodic moisture controls on plant and microbial contributions to soil respiration. *Oecologia*, **167**, 265–278.

Cescatti A, Marcolla B, Santhana SK *et al*. (2012) Remote sensing of environment intercomparison of MODIS albedo retrievals and *in situ* measurements across the global FLUXNET network. *Remote Sensing of Environment*, **121**, 323–334.

Cook BD, Davis KJ, Wang W *et al*. (2004) Carbon exchange and venting anomalies in an upland deciduous forest in northern Wisconsin, USA. *Agricultural and Forest Meteorology*, **126**, 271–295.

CurielYuste J, Janssens IA, Carrara A, Ceulemans R (2004) Annual Q10 of soil respiration reflects plant phenological patterns as well as temperature sensitivity. *Global Change Biology*, **10**, 161–169.

Davidson E, Holbrook NM (2009) *Is Temporal Variation of Soil Respiration Linked to the Phenology of Photosynthesis?* (ed. Noormets A). Springer New York, NY, USA.

Davidson EA, Janssens IA (2006) Temperature sensitivity of soil carbon decomposition and feedbacks to climate change. *Nature*, **440**, 165–173.

Davidson EA, Janssens IA, Luo Y (2006) On the variability of respiration in terrestrial ecosystems: moving beyond Q10. *Global Change Biology*, **12**, 154–164.

DeForest JL, Noormets A, McNulty SG, Sun G, Tenney G, Chen J (2006) Phenophases alter the soil respiration-temperature relationship in an oak-dominated forest. *International Journal of Biometeorology*, **51**, 135–144.

DeForest JL, Chen J, McNulty SG (2009) Leaf litter is an important mediator of soil respiration in an oak-dominated forest. *International Journal of Biometeorology*, **53**, 127–134.

Delpierre N, Soudani K, Francois C *et al*. (2009) Exceptional carbon uptake in European forests during the warm spring of 2007: a data-model analysis. *Global Change Biology*, **15**, 1455–1474.

Dickmann DI, Kozlowski TT (1970) Photosynthesis by rapidly expanding green strobili of Pinus resinosa. *Life Sciences*, **9**, 549–552.

Edwards NT, Hanson PJ (1996) Stem respiration in a closed-canopy upland oak forest. *Tree Physiology*, **16**, 433–439.

Efron B, Tibshirani R (1993) An Introduction to the Bootstrap, New York.

Epron D, Le Dantec V, Dufrene E, Granier A (2001) Seasonal dynamics of soil carbon dioxide efflux and simulated rhizosphere respiration in a beech forest. *Tree Physiology*, **21**, 145–152.

Giasson MA, Ellison AM, Bowden RD *et al*. (2013) Soil respiration in a northeastern US temperate forest: a 22-year synthesis. *Ecosphere* **4.11**. art140. http://dx.doi.org/10.1890/ES13.00183.1

Gobron N, Pinty B, Verstraete MM, Widlowski J-L (2000) Advanced vegetation indices optimized for up-coming sensors: design, performance, and applications. *IEEE T. Geoscience and Remote Sensing*, **38**, 2489–2505.

Gobron N, Pinty B, Aussedat O *et al*. (2006) Evaluation of fraction of absorbed photosynthetically active radiation products for different canopy radiation transfer regimes: methodology and results using joint research center products derived from SeaWiFS against ground-based estimations. *Journal of Geophysical Research*, **111**, D13110.

Golyandina N, Nekrutkin V, Zhigljavsky A (2001) Analysis of time series structure: SSA and related techniques. In: *Monographs on Statistics and Applied Probability*, Vol **90**, CRC Press, Boca Raton, FL, USA.

Gough CM, Vogel CS, Schmid HP, Su H-B, Curtis PS (2008) Multi-year convergence of biometric and meteorological estimates of forest carbon storage. *Agricultural and Forest Meteorology*, **148**, 158–170.

Granier A, Ceschia E, Damesin C *et al*. (2000) The carbon balance of a young Beech forest. *Functional Ecology*, **14**, 312–325.

Gu L, Meyers T, Pallardy SG *et al*. (2006) Direct and indirect effects of atmospheric conditions and soil moisture on surface energy partitioning revealed by a prolonged drought at a temperate forest site. *Journal of Geophysical Research*, **111**, D16102.

Hansen MC, Defries RS, Townshend JRG, Sohlberg R (2000) Global land cover classification at 1 km spatial resolution using a classification tree approach. *International Journal of Remote Sensing*, **21**, 1331–1364.

Hendrick RL, Pregitzer KS (1996) Temporal and depth-related patterns of fine root dynamics in northern hardwood forests. *Journal of Ecology*, **84**, 167–176.

Irvine J, Law BE, Martin JG, Vickers D (2008) Interannual variation in soil CO2 efflux and the response of root respiration to climate and canopy gas exchange in mature ponderosa pine. *Global Change Biology*, **14**, 2848–2859.

Janssen PHM, Heuberger PSC (1995) Calibration of process-oriented models. *Ecological Modelling*, **83**, 55–66.

Jenkins JP, Richardson AD, Braswell BH, Ollinger SV, Hollinger DY, Smith M-L (2007) Refining light-use efficiency calculations for a deciduous forest canopy using simultaneous tower-based carbon flux and radiometric measurements. *Agricultural and Forest Meteorology*, **143**, 64–79.

Joslin J, Wolfe M, Hanson P (2001) Factors controlling the timing of root elongation intensity in a mature upland oak stand. *Plant and Soil*, **228**, 201–212.

Jung M, Verstraete M, Gobron N *et al*. (2008) Diagnostic assessment of European gross primary production. *Global Change Biology*, **14**, 2349–2364.

Knohl A, Schulze E-D, Kolle O, Buchmann N (2003) Large carbon uptake by an unmanaged 250-year-old deciduous forest in Central Germany. *Agricultural and Forest Meteorology*, **118**, 151–167.

Kondrashov D, Ghil M (2006) Spatio-temporal filling of missing points in geophysical data sets. *Nonlinear Processes in Geophysics*, **13**, 151–159.

Korner C, Larcher W (1988) Plant life in cold climates. In: *Plants and Temperature*, Vol **42** (eds Long SP, Woodward FI), pp. 25–57. The Company of Biologists Limited, Cambridge.

Landhäusser SM (2010) Aspen shoots are carbon autonomous during bud break. *Trees*, **25**, 531–536.

Lasslop G, Migliavacca M, Bohrer G *et al*. (2012) On the choice of the driving temperature for eddy-covariance carbon dioxide flux partitioning. *Biogeosciences*, **9**, 5243–5259.

Law BE, Ryan MG, Anthoni PM (1999) Seasonal and annual respiration of a ponderosa pine ecosystem. *Global Change Biology*, **5**, 169–182.

Law BE, Thornton P, Irvine J, Anthoni P, Van Tuyl S (2001) Carbon storage and fluxes in ponderosa pine forests at different developmental stages. *Global Change Biology*, **7**, 755–777.

Le Maire G, Delpierre N, Jung M *et al*. (2010) Detecting the critical periods that underpin interannual fluctuations in the carbon balance of European forests. *Journal of Geophysical Research G: Biogeosciences*, **115**, G00H03.

Lieth H (1974) *Phenology and Seasonality Modelling*, vol **8**, Springer, Heidelberg.

Liu HP, Randerson JT, Lindfors J, Chapin FS (2005) Changes in the surface energy budget after fire in boreal ecosystems of interior Alaska: an annual perspective. *Journal of Geophysical Research*, **110**, D13101.

Lloyd J, Taylor JA (1994) On the temperature dependence of soil respiration. *Functional Ecology*, **8**, 315–323.

Ludwig LJ, Charles-Edwards DA, Withers AC (1994) Tomato leaf photosynthesis and respiration in various light and carbon dioxide environments. In: *Environmental and Biological Control of Photosynthesis* (ed. Marcelle R), pp. 29–36. Springer, the Netherlands.

Mahecha MD, Reichstein M, Lange H *et al*. (2007) Characterizing ecosystem-atmosphere interactions from short to interannual time scales. *Biogeosciences*, **4**, 743–758.

Mahecha MD, Reichstein M, Carvalhais N *et al*. (2010a) Global convergence in the temperature sensitivity of respiration at ecosystem level. *Science*, (New York, N.Y.) **329**, 838–840.

Mahecha MD, Reichstein M, Jung M *et al*. (2010b) Comparing observations and process-based simulations of biosphere-atmosphere exchanges on multiple timescales. *Journal of Geophysical Research G: Biogeosciences*, **115**, G02003.

Migliavacca M, Meroni M, Manca G *et al*. (2009) Seasonal and interannual patterns of carbon and water fluxes of a poplar plantation under peculiar eco-climatic conditions. *Agricultural and Forest Meteorology*, **149**, 1460–1476.

Migliavacca M, Reichstein M, Richardson AD *et al*. (2011) Semiempirical modeling of abiotic and biotic factors controlling ecosystem respiration across eddy covariance sites. *Global Change Biology*, **17**, 390–409.

Misson L, Gershenson A, Tang J, Mckay M, Cheng W, Goldstein A (2006) Influences of canopy photosynthesis and summer rain pulses on root dynamics and soil respiration in a young ponderosa pine forest. *Tree Physiology*, **26**, 833–844.

Morecroft MD, Stokes VJ, Morison JIL (2003) Seasonal changes in the photosynthetic capacity of canopy oak (Quercus robur) leaves: the impact of slow development on annual carbon uptake. *International Journal of Biometeorology*, **47**, 221–226.

Papale D, Reichstein M, Aubinet M *et al*. (2006) Towards a standardized processing of net ecosystem exchange measured with eddy covariance technique: algorithms and uncertainty estimation. *Biogeosciences*, **3**, 571–583.

Peel MC, Finlayson BL, McMahon TA (2007) Updated world map of the Köppen–Geiger climate classification. *Hydrology and Earth System Science*, **11**, 1633–1644.

Peichl M, Sonnentag O, Wohlfahrt G *et al*. (2013) Convergence of potential net ecosystem production among contrasting C3 grasslands. *Ecology Letters*, **16**, 502–512.

Peters-Lidard CD, Mocko DM, Garcia M, Santanello JA Jr, Tischler MA, Moran MS, Wu Y (2008) Role of precipitation uncertainty in the estimation of hydrologic soil properties using remotely sensed soil moisture in a semiarid environment. *Water Resource Research*, **44**, W05S18.

Raich JW, Potter CS, Bhagawati D (2002) Interannual variability in global soil respiration, 1980–1994. *Global Change Biology*, **8**, 800–812.

Reichstein M, Rey A, Freibauer A *et al*. (2003) Modeling temporal and large-scale spatial variability of soil respiration from soil water availability, temperature and vegetation productivity indices. *Global Biogeochemical Cycles*, **17**, 11–15.

Reichstein M, Falge E, Baldocchi D *et al*. (2005) On the separation of net ecosystem exchange into assimilation and ecosystem respiration: review and improved algorithm. *Global Change Biology*, **11**, 1424–1439.

Reichstein M, Beer C (2008) Soil respiration across scales: the importance of a model-data integration framework for data interpretation. *Journal of Plant Nutrition and Soil Science*, **171**, 344–354.

Richardson AD, Braswell BH, Hollinger DY *et al*. (2006) Comparing simple respiration models for eddy flux and dynamic chamber data. *Agricultural and Forest Meteorology*, **141**, 219–234.

Schmid H, Grimmond C, Cropley F (2000) Measurements of CO2 and energy fluxes over a mixed hardwood forest in the mid-western United States. *Agricultural and Forest Metrology*, **103**, 357–374.

Sprugel DG, Ryan MR, Brooks JR, Vogt KA, Martin TA (1995) Respiration from the organ to the stand. In: *Resource Physiology of Conifers* (eds Smith W, Hinckley T), pp. 225–299. Academic Press, New York, NY, USA.

Subke J-A, Bahn M (2010) On the 'temperature sensitivity' of soil respiration: can we use the immeasurable to predict the unknown? *Soil Biology and Biochemistry*, **42.9**, 1653–1656.

Trumbore S (2006) Carbon respired by terrestrial ecosystems – recent progress and challenges. *Global Change Biology*, **12**, 141–153.

Urbanski S, Barford C, Wofsy S *et al*. (2007) Factors controlling CO2 exchange on timescales from hourly to decadal at Harvard Forest. *Journal of Geophysical Research-Biogeosciences*, **112**, G02020.

Wilson BF, Batchelard EP (1975) Effects of girdling and defoliation on root elongation intensity and survival of Eucalyptus regnans and *E. viminalis* seedlings. *Australian Journal of Plant Physiology*, **2**, 197–206.